Biochimica et Biophysica Acta 1811 (2011) 1011–1020

Contents lists available at SciVerse ScienceDirect

Biochimica et Biophysica Acta

journal homepage: www.elsevier.com/locate/bbalip

Lack of acyl-CoA:diacylglycerol acyltransferase 1 reduces intestinal cholesterol absorption and attenuates atherosclerosis in apolipoprotein E knockout mice

Prakash G. Chandak [a], Sascha Obrowsky [a], Branislav Radovic [a], Prakash Doddapattar [a], Elma Aflaki [a,1], Adelheid Kratzer [a,2], Lalit S. Doshi [a], Silvia Povoden [a], Helmut Ahammer [b], Gerald Hoefler [c], Sanja Levak-Frank [a], Dagmar Kratky [a,*]

[a] Institute of Molecular Biology and Biochemistry, Center of Molecular Medicine, Medical University of Graz, Harrachgasse 21, 8010 Graz, Austria
[b] Institute of Biophysics, Medical University of Graz, Harrachgasse 21, 8010 Graz, Austria
[c] Institute of Pathology, Medical University of Graz, Auenbruggerplatz 25, 8036 Graz, Austria

ARTICLE INFO

Article history:
Received 7 April 2011
Received in revised form 28 July 2011
Accepted 15 August 2011
Available online 1 September 2011

Keywords:
Atherosclerosis
Cholesterol absorption
Cholesterol efflux
Acyl-CoA:diacylglycerol acyltransferase 1
Inflammation
Apolipoprotein E knockout mice

ABSTRACT

Triacylglycerols (TG) are the major storage molecules of metabolic energy and fatty acids in several tissues. The final step in TG biosynthesis is catalyzed by acyl-CoA:diacylglycerol acyltransferase (DGAT) enzymes. Lack of whole body DGAT1 is associated with reduced lipid-induced inflammation. Since one major component of atherosclerosis is chronic inflammation we hypothesized that DGAT1 deficiency might ameliorate atherosclerotic lesion development. We therefore crossbred Apolipoprotein E-deficient ($ApoE^{-/-}$) mice with $Dgat1^{-/-}$ mice. $ApoE^{-/-}$ and $ApoE^{-/-}Dgat1^{-/-}$ mice were fed Western-type diet (WTD) for 9 weeks and thereafter examined for plaque formation. The mean atherosclerotic lesion area was substantially reduced in $ApoE^{-/-}Dgat1^{-/-}$ compared with $ApoE^{-/-}$ mice in *en face* and aortic valve section analyses. The reduced lesion size was associated with decreased cholesterol uptake and absorption by the intestine, reduced plasma TG and cholesterol concentrations and increased cholesterol efflux from macrophages. The expression of adhesion molecules was reduced in aortas of $ApoE^{-/-}Dgat1^{-/-}$ mice, which might be the reason for less migration capacities of monocytes and macrophages and the observed decreased amount of macrophages within the plaques. From our results we conclude that the lack of DGAT1 is atheroprotective, implicating an additional application of DGAT1 inhibitors with regard to maintaining cholesterol homeostasis and attenuating atherosclerosis.

© 2011 Elsevier B.V. Open access under CC BY-NC-ND license.

1. Introduction

In mammalian cells, neutral lipids including cholesteryl esters and triacylglycerols (TG) form lipid droplets as storage organelles. TG are the major storage molecules of metabolic energy and fatty acids (FAs) in most cells and tissues. The final step in TG biosynthesis is catalyzed by acyl-CoA:diacylglycerol acyltransferase (DGAT) enzymes. In mice, DGAT1 is expressed ubiquitously with highest mRNA levels in the small intestine, testis, adipose tissue, and mammary gland [1]. DGAT2 is expressed in adipose tissue, liver and many other tissues, including cardiac muscle, small intestine, skeletal muscle, and kidney [2]. DGAT2 is speculated to be closely linked to endogenous FA biosynthesis and esterification, whereas DGAT1 might be involved in the recycling of hydrolyzed TG by reesterifying the FAs [3]. DGAT2 deficiency in mice causes early postnatal lethality and a severe decrease in carcass TG content [4]. Dgat1-deficient ($Dgat1^{-/-}$) mice are lean, resistant to diet-induced obesity and show substantially decreased DGAT activity in several tissues [5]. Reduced body weight in $Dgat1^{-/-}$ mice correlates with an increased rate of energy expenditure and a delayed transit of TG through the enterocyte into the circulation [6]. Whole-body DGAT1 deficiency was associated with reduced inflammation in adipose tissue, whereas DGAT1 deficiency in isolated macrophages increased the propensity of FA-induced inflammation [7]. It has recently been shown that obesity resistance of $Dgat1^{-/-}$ mice was due to the absence of intestinal DGAT1 expression [8]. aP2-*Dgat1* transgenic mice with increased DGAT1 levels in adipocytes and macrophages were prone to diet-induced obesity but were protected against non-adipose tissue steatosis and systemic inflammation [7].

Since atherosclerosis is an inflammatory disease our study was designed to investigate the consequences of whole-body DGAT1 deficiency on atherosclerosis susceptibility. Atherosclerosis is characterized by lipid accumulation and an inflammatory response in the

Abbreviations: ApoE, apolipoprotein E; DGAT, acyl-CoA:diacylglycerol acyltransferase; FA, fatty acids; FFA, free fatty acids; FC, free cholesterol; TC, total cholesterol; TG, triacylglycerol; WTD, western-type diet

* Corresponding author. Tel.: +43 3163807543.
E-mail address: dagmar.kratky@medunigraz.at (D. Kratky).
[1] Present address: National Human Genome Research Institute, 35 Convent Dr., Bethesda, MD 20892, USA.
[2] Present address: Division of Pulmonary and Critical Care, University of Colorado Denver, Anschutz Medical Campus 12700, Denver, CO 80045, USA.

1388-1981 © 2011 Elsevier B.V. Open access under CC BY-NC-ND license.
doi:10.1016/j.bbalip.2011.08.010

arterial intima resulting in plaque formation [9,10]. Sites of inflammation attract monocytes, which adhere to the endothelium with the help of certain adhesion molecules. Monocytes enter the intima through the endothelium and acquire morphological characteristics of macrophages by increasing the expression of scavenger receptor A (SRA) and cluster of differentiation 36 (CD36). As a consequence, macrophages internalize modified lipoproteins and accumulate cholesteryl esters that ultimately lead to foam cell formation, a characteristic of early atherosclerotic lesions. To study the involvement of DGAT1 in atherogenesis, *Dgat1*$^{-/-}$ mice [5] were cross-bred with Apolipoprotein E (*ApoE*)$^{-/-}$ mice, an atherosclerosis-susceptible strain with impaired clearance of ApoB-containing lipoproteins [11,12]. We observed substantially reduced plaque formation in *ApoE*$^{-/-}$*Dgat1*$^{-/-}$ mice compared with *ApoE*$^{-/-}$ mice. Our results suggest that the protection against atherosclerosis is multifactorial, including reduced aortic inflammation and adaptive changes in intestinal and macrophage cholesterol metabolism.

2. Theory

Dgat1$^{-/-}$ mice are resistant to diet-induced obesity and fatty liver disease, exhibit increased energy expenditure, preserve insulin and leptin sensitivity, and are resistant to FA-induced inflammation. DGAT1 inhibitors were shown to induce weight loss and improve insulin sensitivity, glucose tolerance and lipid levels in obese mice, suggesting that these compounds may be beneficial in the treatment of obesity, diabetes and dyslipidemia. Since DGAT1 deficiency is linked with phenotypic components that are generally associated with reduced atherosclerosis susceptibility we hypothesized that DGAT1 deficiency attenuates atherosclerotic plaque formation in *ApoE*$^{-/-}$ mice.

3. Materials and methods

3.1. Animals

Dgat1$^{-/-}$ [5] and *ApoE*$^{-/-}$ mice (The Jackson Laboratory, Bar Harbor, ME, USA) were crossed to yield *ApoE*$^{-/-}$*Dgat1*$^{-/-}$ mice. All mice were housed in sterilized filter-top cages and given unlimited access to food and water. The mice were maintained on regular chow diet, containing 4.3% (w/w) fat with no added cholesterol (Ssniff, Soest, Germany) on a regular 12 h dark/light cycle. At the age of 6–8 weeks, female *ApoE*$^{-/-}$*and ApoE*$^{-/-}$*Dgat1*$^{-/-}$ mice were challenged with a Western-type diet (WTD; 21% fat, 0.4% cholesterol; Ssniff) for 9 weeks to induce atherosclerotic lesion development. All experimental protocols were approved by the Austrian Federal Ministry of Science and Research, Division of Genetic Engineering and Animal Experiments (Vienna, Austria).

3.2. Lipid analyses in plasma and small intestines

Blood was collected by retro-orbital venous plexus puncture after an overnight fasting period. TG, free cholesterol (FC) (both from DiaSys, Holzheim, Germany) and total cholesterol (TC) (Greiner Diagnostics AG, Bahlingen, Germany) concentrations were determined spectrophotometrically. Free fatty acid (FFA) concentrations were assayed using a NEFA FS kit (DiaSys, Holzheim, Germany) according to the manufacturer's protocol. Bile acid concentrations in the plasma were determined in the fed state *in ApoE*$^{-/-}$ and *ApoE*$^{-/-}$*Dgat1*$^{-/-}$ mice fed with WTD for 9 weeks (DiaSys, Holzheim, Germany). To analyze lipid parameters in the small intestine, *ApoE*$^{-/-}$ and *ApoE*$^{-/-}$*Dgat1*$^{-/-}$ mice were fed with WTD for 4 weeks. After a fasting period of 4 h the middle part of the small intestine (jejunum) was collected. The lipids were extracted by the addition of 2 ml hexane: isopropanol (3:2, v:v) for 1 h at 4 °C. The lipid extract was dried under a stream of nitrogen. One hundred microliters 1% Triton-X100 in chloroform was added and dried again under nitrogen. Thereafter, the samples were dissolved in 100 µl dH_2O, and TG and TC concentrations were measured using above mentioned kits. The readings were normalized to protein concentrations.

3.3. Lipoprotein profiles

ApoE$^{-/-}$ and *ApoE*$^{-/-}$*Dgat1*$^{-/-}$ mice were fed chow diet. Mice were fasted for 4 h and plasma was isolated. A pool of 200 µl per genotype was subjected to fast protein liquid chromatography (FPLC) on a Pharmacia FPLC system (Pfizer Pharma, Karlsruhe, Germany) equipped with a Superose 6 column (Amersham Biosciences, Piscataway, NJ). The lipoproteins were eluted with 10 mM Tris–HCl, 1 mM EDTA, 0.9% NaCl, and 0.02% NaN3 (pH 7.4). Fractions of 0.5 ml each were collected and TG and TC concentrations were assayed enzymatically using above mentioned kits. To enhance sensitivity, reaction buffers were supplemented by the addition of sodium 3,5-dichloro-2-hydroxy-benzenesulfonate.

3.4. Preparation of histological sections and lesion analysis

Atherosclerotic lesions in aortic root and aorta of *ApoE*$^{-/-}$ and *ApoE*$^{-/-}$*Dgat1*$^{-/-}$ mice were analyzed after 9 weeks feeding the WTD. Mice were euthanized and then the arterial tree was perfused in situ with PBS (100 mm Hg) for 10 min via a cannula in the left ventricular apex. Liver and small intestine were collected and mice were perfused with 4% neutral-buffered formalin (Carl Roth GmbH, Vienna, Austria) for 15 min. After fixing hearts, livers and intestines in 4% neutral-buffered formalin, serial sections (8 µm) were cut (HM 560 Cryo-Star; Microm International GmbH, Walldorf, Germany). Images of the atherosclerotic lesion areas in oil red-O (Sigma-Aldrich, St. Louis, MO) stained sections were taken with ScanScope T3 whole slide scanner (Aperio Technologies, Bristol, UK). Plaque areas were quantitated by ImageJ software and a software algorithm which had been programmed with Interactive Data Language (IDL, ITT Visual Information Solutions, Boulder, USA) [13]. Mean lesion area was calculated from 10 consecutive oil red O-stained sections, starting at the appearance of the tricuspid valves. Sections were stained immunohistochemically for the presence of macrophages using a monoclonal rat anti-mouse Moma-2 antibody (1:600) (Acris, Hiddenhausen, Germany).

For *en face* analysis, aortas were dissected and plaques were stained with oil red O as described recently [13]. Images were analyzed using ImageJ software. Images of oil red O-stained liver and intestine sections were taken with a Nikon Eclipse 80i microscope (Nikon, Vienna, Austria).

3.5. Cell culture

Macrophages were isolated from the peritoneum of *ApoE*$^{-/-}$ and *ApoE*$^{-/-}$*Dgat*$^{-/-}$ mice 3 days after intraperitoneal injection of 3 ml 3% thioglycolate medium. Cells were washed three times with PBS and cultivated in Dulbecco's modified Eagle's medium (DMEM), 10% lipoprotein-deficient serum (LPDS), 100 µg/ml penicillin/streptomycin in the absence and presence of 100 µg/ml acetylated (ac)LDL for 24 h. LDL and HDL were isolated from human plasma by density gradient ultracentrifugation and LDL was acetylated as described [14]. Protein was quantitated using a Bradford assay (Bio-Rad Laboratories, Hercules, CA).

3.6. DiI-acLDL and DiI-VLDL uptake

Macrophages were cultured in DMEM/10% LPDS in 12-well culture plates for 24 h. Thereafter, cells were incubated in serum-free DMEM with 10 µg/ml 1,1′-dioctadecyl-3,3,3′,3′-tetramethylindocarbocyanine perchlorate (DiI)-acLDL and 50 µg/ml DiI-VLDL for 4 h. Cells were washed thrice with PBS, detached by scraping, stained with F4/80

(1:250) (BD Biosciences, San Jose, CA) and IgG_2 as isotype control and analyzed by fluorescence activated cell sorting (FACS) (FACSCalibur; BD Biosciences, San Jose, CA).

3.7. Cellular cholesterol efflux

Macrophages were incubated with 100 μg 0.5 μCi/ml ^{3}H-cholesterol (ARC Inc., St. Louis, MO) and 30 μg/ml non-labeled cholesterol in DMEM/0.2% FA-free BSA for 32 h at 37 °C. After washing the cells twice with PBS, the cells were incubated for 16 h in equilibration medium (DMEM/0.2% FA-free BSA in the absence or presence of 0.3 mM 8-bromo-cAMP (Sigma-Aldrich, St. Louis, MO)). We determined cholesterol efflux after incubating the cells in DMEM/0.2% FA-free BSA in the absence or presence of 15 μg/ml ApoA-I (Calbiochem, La Jolla, CA) or 100 μg/ml HDL_3. Radioactivity in 100 μl medium and in the cells was measured by scintillation counting after 1, 3, 6, and 9 h of incubation. Cholesterol efflux is expressed as the percentage of total cell ^{3}H-cholesterol present in the medium after 1, 3, 6, and 9 h. Basal efflux in the absence of ApoA-I and HDL_3 was subtracted from the data shown.

3.8. Migration assay

We assessed cell migration using ~2 million peritoneal macrophages or bone marrow monocytes loaded into the upper wells of 24-well transwell plates (macrophages: 5 μm pore size; monocytes: 3 μm pore size; Corning, Lowell, MA). The lower chambers were filled with 600 μl DMEM containing monocyte chemoattractant protein 1 (MCP-1, 50 ng/ml). The amount of monocytes and macrophages in the lower chambers were determined after 4 h at 37 °C by FACS (FACSCalibur; BD Biosciences, San Jose, CA). The chemotactic index was calculated as the ratio of cells that had moved from the top to the lower chamber in the presence or absence of MCP-1.

3.9. Nile red staining and fluorescence microscopy

We plated macrophages from chow or WTD-fed *ApoE*$^{-/-}$ and *ApoE*$^{-/-}$*Dgat1*$^{-/-}$ mice on chamber slides in serum-free DMEM for 24 h, fixed them with paraformaldehyde and stained the lipid droplets with Nile red [15]. Lipid droplets were visualized by confocal laser scanning microscopy as described previously [15] using an LSM 510 META microscope system (Carl Zeiss GmbH, Vienna, Austria).

3.10. mRNA expression analysis by real time PCR

Total RNA from aortas and intestines was isolated using TriFast (Peqlab, Erlangen, Germany). Total RNA from macrophages was isolated using peqGOLD kit (Peqlab, Erlangen, Germany). RNA was reverse transcribed using the High Capacity cDNA Reverse Transcription Kit (Applied Biosystems, Foster City, CA). Quantitative real time PCR was performed on a LightCycler 480 system (Roche, Basel, Switzerland) using the Quantifast SYBR Green PCR kit (Qiagen, Hilden, Germany). Data are displayed as expression ratios of target genes normalized to the expression of cyclophilin A as internal reference in each sample. Data were analyzed using the 2^{-ddCt} method. Primer sequences are available upon request.

3.11. Western blotting

Macrophages from *ApoE*$^{-/-}$ and *ApoE*$^{-/-}$*Dgat1*$^{-/-}$ mice were cultured in DMEM/10% LPDS and incubated with acLDL (100 μg/ml) for 24 h. Macrophages were lysed and 40 μg of protein lysates were separated by 15% SDS-PAGE. After transfer onto nitrocellulose protran BA85 membranes (Whatman, Vienna, Austria), membranes were blocked with 5% BSA for 2 h and incubated with rabbit polyclonal antibodies to murine ABCA1 (1:1000), ABCG1 (1:500), SRB-1 (1:1000) (Acris, Hiddenhausen, Germany), and a monoclonal anti-mouse β-actin (1:5000) (Santa Cruz Biotechnology, Heidelberg, Germany). The horseradish peroxidase-conjugated goat anti-rabbit (1:5000) (Santa Cruz Biotechnology) and rabbit anti-mouse antibodies (Dako, Glostrup, Denmark) were visualized by enhanced chemiluminescence detection (ECL Plus, GE Healthcare, Piscataway, NJ) on an AGFA Curix Ultra X-ray film.

3.12. MCP-1 ELISA

Blood was drawn from WTD-fed *ApoE*$^{-/-}$ and *ApoE*$^{-/-}$*Dgat1*$^{-/-}$ mice. Serum MCP-1 concentrations were determined by ELISA (R&D Systems Inc., Minneapolis, MN) according to the manufacturer's protocol.

3.13. DGAT activity

DGAT activity was determined as described by Buhman et al. [6] with minor modifications. Briefly, TG formation in 50 μg macrophage lysates was measured using 200 μM sn-1,2-dioleoylglycerol (Sigma-Aldrich, St. Louis, MO) and 25 μM ^{14}C-oleoyl-CoA (ARC Inc., St. Louis, MO) as substrates and 10 mM $MgCl_2$. After 5 min of incubation at 37 °C, lipids were extracted with chloroform:methanol (2:1, v:v). The organic layer was dried under nitrogen and redissolved in human serum and chloroform:methanol (1:1, v:v). Lipids were separated by thin layer chromatography in hexane:diethyl ether:acetic acid (79:20:1). TG-specific bands were scraped and the radioactivity was measured by liquid scintillation counting.

3.14. Cholesterol absorption and cholesterol synthesis

We determined acute cholesterol uptake and absorption in overnight fasted *ApoE*$^{-/-}$ and *ApoE*$^{-/-}$*Dgat1*$^{-/-}$ mice. Mice were gavaged with 200 μl corn oil containing 2 μCi 1,2-^{3}H(N)-cholesterol (ARC Inc., St Louis, MO) and 0.2 mg cholesterol. After 4 h, plasma, liver and small intestine were isolated. The small intestine was rinsed with PBS to remove luminal contents. The tissues were dissolved in 1 M NaOH at 65 °C overnight and then analyzed by liquid scintillation counting. We determined the amount of ^{3}H-cholesterol in HDL after precipitation of ApoB-containing lipoproteins with Quantolip HDL (Technoclone GmbH, Vienna, Austria). Plasma samples from each genotype were pooled, 200 μl were subjected to FPLC and the radioactivity in 0.5 ml fractions was determined by liquid scintillation counting. Cholesterol synthesis in *ApoE*$^{-/-}$ and *ApoE*$^{-/-}$*Dgat1*$^{-/-}$ mice after injecting 200 μl PBS containing 5 μCi ^{14}C-acetate (ARC Inc., St Louis, MO) was assessed as described [16].

Dual fecal sterol loss was determined as described previously [17] with minor modifications. Briefly, mice were gavaged with 0.1 μCi ^{14}C-cholesterol and 0.2 μCi ^{3}H-sitosterol (ARC Inc., St Louis, MO) in 200 μl corn oil, and feces were collected for 48 h. Lipids were extracted from feces using the Folch extraction method and radioactivity was determined by liquid scintillation counting. Fractional cholesterol absorption was calculated by the following formula: dose [^{14}C]:[^{3}H] − fecal [^{14}C]:[^{3}H])/dose [^{14}C]:[^{3}H].

3.15. Statistics

Statistical analyses were performed with GraphPad Prism 5.0 software. The significance of paired data was determined by Student's *t*-test. Data with more than 2 groups or 2 independent variables were analyzed by ANOVA followed by the Bonferroni post-hoc test. Data are presented as mean values ± SEM. The probability level for statistical significance was set at $p<0.05$ (*), $p\leq0.01$ (**) and $p\leq0.001$ (***).

4. Results

4.1. Reduced plasma lipid concentrations in *ApoE*$^{-/-}$*Dgat1*$^{-/-}$ mice

First, we determined plasma lipid parameters of 6–8 week old female *ApoE*$^{-/-}$ and *ApoE*$^{-/-}$*Dgat1*$^{-/-}$ mice fed chow diet. We found significantly reduced concentrations of TG (30%), FFA (27%) and FC (17%) in *ApoE*$^{-/-}$*Dgat1*$^{-/-}$ compared with *ApoE*$^{-/-}$ mice, whereas total cholesterol (TC) and cholesteryl ester (CE) concentrations remained unchanged (Table 1). To investigate the effect of DGAT1 deficiency on early atherosclerosis, *ApoE*$^{-/-}$ and *ApoE*$^{-/-}$*Dgat1*$^{-/-}$ mice were fed WTD for 9 weeks. Animals from both genotypes exhibited similar body weights before (14–15 g) and after feeding the WTD (20–21 g) (supplemental Fig. S1). Plasma TG and FFA concentrations were significantly decreased in WTD-fed *ApoE*$^{-/-}$*Dgat1*$^{-/-}$ compared with *ApoE*$^{-/-}$ mice (Table 1). In addition, WTD feeding resulted in a 20% reduction in plasma TC levels and a concomitant 26% decrease in FC concentrations (Table 1). Plasma CE concentrations remained unchanged in *ApoE*$^{-/-}$*Dgat1*$^{-/-}$ compared with *ApoE*$^{-/-}$ mice, suggesting that the particle types are unaltered.

4.2. Reduced plaque formation in *ApoE*$^{-/-}$*Dgat1*$^{-/-}$ mice

To study the impact of DGAT1 deficiency on atherosclerosis susceptibility of *ApoE*$^{-/-}$ mice, we compared plaque formation in *ApoE*$^{-/-}$*Dgat1*$^{-/-}$ and *ApoE*$^{-/-}$ mice. Quantification of oil red O-stained *en face* preparations of aortas revealed a 36% reduction in plaque area of *ApoE*$^{-/-}$*Dgat1*$^{-/-}$ compared with *ApoE*$^{-/-}$ mice (Fig. 1A). In addition, we observed a 24% decrease of the lesion area in aortic valve sections of *ApoE*$^{-/-}$*Dgat1*$^{-/-}$ mice (Fig. 1B). Immunohistochemical staining of macrophages in aortic valve sections using the macrophage-specific anti-Moma2 antibody demonstrated that the macrophage area in sections of *ApoE*$^{-/-}$*Dgat1*$^{-/-}$ plaques was 27% reduced compared with *ApoE*$^{-/-}$ mice (Fig. 1C).

4.3. Reduced mRNA expression of genes involved in monocyte recruitment and decreased migration of *ApoE*$^{-/-}$*Dgat1*$^{-/-}$ macrophages

To investigate whether the reduction in atherosclerosis observed in *ApoE*$^{-/-}$*Dgat1*$^{-/-}$ mice might directly affect the arterial wall and to elucidate whether primary rather than secondary effects are involved, we isolated the descending aortas and macrophages from chow diet-fed mice. First we determined mRNA levels of several genes known to be responsible for monocyte recruitment and adhesion. We found unchanged mRNA expression of Icam1 but markedly reduced mRNA levels of Vcam1, P-selectin, E-selectin, and Mcp1 in aortas of *ApoE*$^{-/-}$*Dgat1*$^{-/-}$ compared with *ApoE*$^{-/-}$ mice (42%, 35%, 52%, and 38%, respectively) (Fig. 2A). In addition, Vla-4 mRNA levels were 69% reduced in *ApoE*$^{-/-}$*Dgat1*$^{-/-}$ compared with *ApoE*$^{-/-}$ peritoneal macrophages (Fig. 2B). These observations indicate that the lack of DGAT1 might reduce leukocyte infiltration by regulating cell adhesion and transendothelial cell migration. In accordance, by using MCP1 as a chemoattractant, we found markedly decreased migration capacities of peritoneal macrophages and bone marrow-derived *ApoE*$^{-/-}$*Dgat1*$^{-/-}$ monocytes (58% and 68%, respectively) (Fig. 2C). Reduced monocyte/macrophage migration to the site of injury is generally associated with a less inflammatory phenotype. Accordingly, MCP-1 protein levels were decreased by 26% in serum of WTD-fed *ApoE*$^{-/-}$*Dgat1*$^{-/-}$ compared with *ApoE*$^{-/-}$ mice (Fig. 2D). These data suggest that DGAT1 deficiency exhibits functional changes that play an important role in the attenuation of the inflammatory response in atherosclerosis development of *ApoE*$^{-/-}$*Dgat1*$^{-/-}$ mice.

4.4. Increased cholesterol efflux from *ApoE*$^{-/-}$*Dgat1*$^{-/-}$ macrophages

To assess whether reverse cholesterol transport is affected in *ApoE*$^{-/-}$*Dgat1*$^{-/-}$ macrophages *in vitro*, we loaded macrophages from chow diet-fed mice with ^{3}H-cholesterol-labeled acLDL and determined cholesterol efflux to ApoA1 and HDL_3 as extracellular acceptors after 1, 3, 6, and 9 h. Cholesterol efflux was drastically increased in *ApoE*$^{-/-}$*Dgat1*$^{-/-}$ macrophages compared with *ApoE*$^{-/-}$ cells and this effect was even more pronounced after cAMP activation (Fig. 3A–D). To elucidate whether DGAT1 deficiency affects cholesterol efflux also in the presence of ApoE, we determined cholesterol efflux in macrophages from *Dgat1*$^{-/-}$ and Wt mice. As shown in the supplemental Fig. S3, cholesterol efflux to ApoA1 was markedly increased in *Dgat1*$^{-/-}$ compared with Wt mice.

Next we analyzed mRNA levels of genes involved in cholesterol efflux in acLDL-loaded macrophages from *ApoE*$^{-/-}$ and *ApoE*$^{-/-}$*Dgat1*$^{-/-}$ macrophages. We found unchanged Acat1 mRNA expression but increased mRNA levels of Abca1, Abcg1 and Sr-b1 (1.7-, 6.9- and 3.1-fold, respectively) in *ApoE*$^{-/-}$*Dgat1*$^{-/-}$ foam cells (Fig. 3E). Accordingly, ABCA1 and ABCG1 protein expressions were increased in acLDL-loaded macrophages from *ApoE*$^{-/-}$*Dgat1*$^{-/-}$ mice (Fig. 3F). Although no differences were observed in mRNA and protein expression of Abca1, Abcg1 and Sr-b1 in unloaded macrophages the protein expression of ABCG1 and SR-B1 were increased (supplemental Fig. S4A, B).

4.5. Reduced foam cell formation in *ApoE*$^{-/-}$*Dgat1*$^{-/-}$ macrophages

To further investigate the role of macrophages in the reduced atherosclerosis susceptibility of *ApoE*$^{-/-}$*Dgat1*$^{-/-}$ mice, we isolated macrophages from chow-diet fed mice and analyzed them for lipid uptake. The uptake of DiI-labeled acLDL was significantly decreased by 22%, whereas the uptake of DiI-VLDL was only slightly reduced in *ApoE*$^{-/-}$*Dgat1*$^{-/-}$ versus *ApoE*$^{-/-}$ cells (Fig. 4A, B). The mRNA expression of pro-atherosclerotic Sr-a was reduced by 76%, whereas Cd36 levels were unaffected (Fig. 4C). Total DGAT activity was reduced by 64% in *ApoE*$^{-/-}$*Dgat1*$^{-/-}$ compared with *ApoE*$^{-/-}$ macrophages (Fig. 4D). Nile red staining of untreated, acLDL- and VLDL-loaded macrophages showed that the amount of lipid droplets was markedly reduced in cells from *ApoE*$^{-/-}$*Dgat1*$^{-/-}$ compared with *ApoE*$^{-/-}$ mice (Fig. 4E). To analyze the *in vivo* foam cell formation, we isolated macrophages of WTD-fed mice and determined the percentage of cells containing lipid droplets. Macrophages from *ApoE*$^{-/-}$

Table 1
Lipid parameters of age-matched female *ApoE*$^{-/-}$ and *ApoE*$^{-/-}$/*Dgat*$^{-/-}$ mice before and after feeding Western type diet (WTD) for 9 weeks. TG, FFA, TC, and FC concentrations were determined enzymatically and CE concentrations were calculated as CE = TC − FC. Data are expressed as mean values ± SEM. $^{*}p<0.05$; $^{***}p\leq0.001$.

Genotype	*n*	TG (mg/dl)	FFA (mM)	TC (mg/dl)	FC (mg/dl)	CE (mg/dl)
Before WTD						
ApoE$^{-/-}$	9	110 ± 13	1.47 ± 0.109	322 ± 14	105 ± 2.2	217 ± 13
ApoE$^{-/-}$/*Dgat*$^{-/-}$	11	76.5 ± 7.5*	1.07 ± 0.137*	290 ± 24	87.5 ± 5.7*	203 ± 19
After WTD						
ApoE$^{-/-}$	9	270 ± 10	1.74 ± 0.093	905 ± 27	471 ± 18	434 ± 15
ApoE$^{-/-}$/*Dgat*$^{-/-}$	11	159 ± 8.8***	1.18 ± 0.055***	735 ± 35***	337 ± 18***	398 ± 19

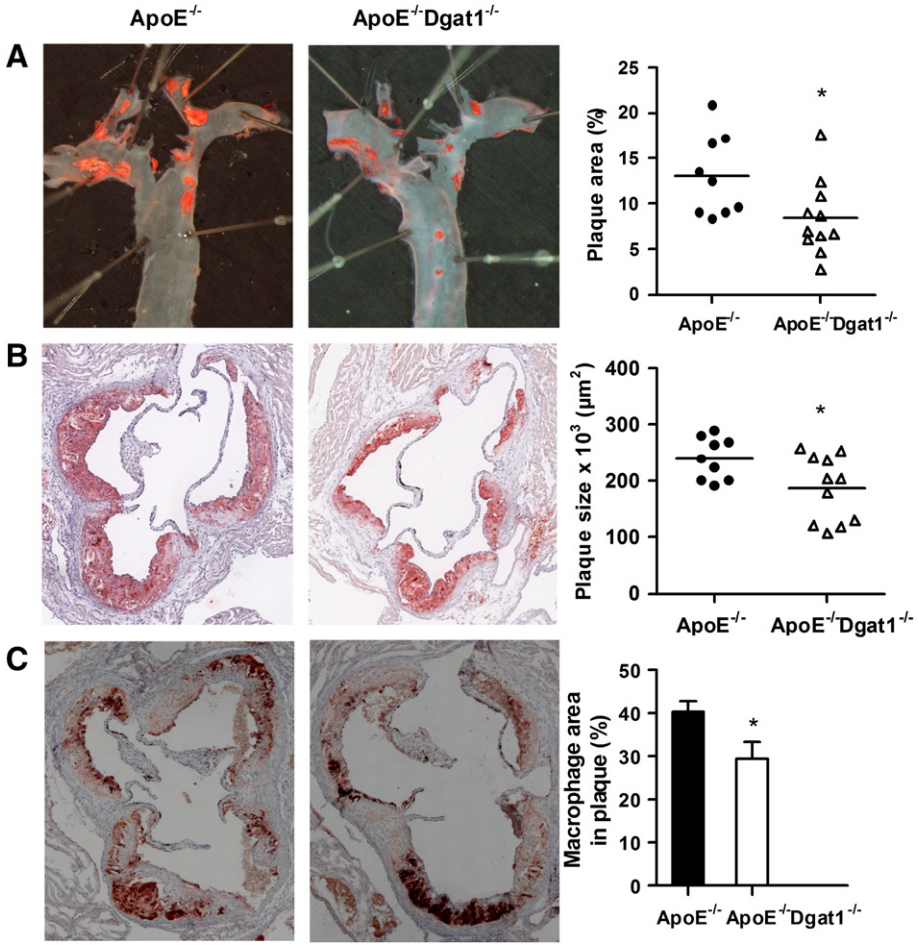

Fig. 1. Reduced plaque formation in *ApoE*$^{-/-}$*Dgat1*$^{-/-}$ mice. Female *ApoE*$^{-/-}$ and *ApoE*$^{-/-}$*Dgat1*$^{-/-}$ mice were fed WTD for 9 weeks. Representative images and quantifications of (A) oil red O-stained *en face* aorta and of aortic valve sections stained with (B) oil red O and (C) macrophage-specific anti-Moma2 antibody. (A) Data represent means ($n = 9$–11) of the quantification of plaque formation. (B) Data represent the mean values of 10 aortic valve sections per mouse. Bars represent the mean values of 9–11 animals per group. C, Mean values of 5 sections from 6 to 7 mice ± SEM are shown. $^{*}p < 0.05$.

Dgat1$^{-/-}$ mice had 30% less lipid droplet-containing cells compared with cells from *ApoE*$^{-/-}$ mice (Fig. 4F). These data indicate that DGAT1 is required for efficient foam cell formation of *ApoE*$^{-/-}$ macrophages and that its absence reduces lipid droplet accumulation.

4.6. Reduced cholesterol uptake and absorption in *ApoE*$^{-/-}$*Dgat1*$^{-/-}$ mice

We observed a reduced number of lipid droplets in livers of WTD-fed *ApoE*$^{-/-}$*Dgat1*$^{-/-}$ compared with *ApoE*$^{-/-}$ mice (Fig. 5A). In contrast, intestines of *ApoE*$^{-/-}$*Dgat1*$^{-/-}$ mice exhibited a markedly increased amount of lipid droplets when compared to *ApoE*$^{-/-}$ mice (Fig. 5B) with elevated intestinal TC and TG concentrations (Fig. 5C). These data indicate that TG and cholesterol accumulate within enterocytes of *ApoE*$^{-/-}$*Dgat1*$^{-/-}$ mice. In line with these data, we observed reduced plasma cholesterol concentrations in *ApoE*$^{-/-}$*Dgat1*$^{-/-}$ compared with *ApoE*$^{-/-}$ mice (Table 1), whereas plasma bile acid concentrations were unchanged (supplemental Fig. S5).

DGAT1 inhibitor treatment reduced plasma cholesterol levels in genetically obese KKA^{y} mice [18]. The authors suggested that this was mainly due to a decrease in intestinal cholesterol absorption and/or reduction of hepatic cholesterol synthesis. We therefore determined intestinal cholesterol uptake and absorption in chow-fed *ApoE*$^{-/-}$*Dgat1*$^{-/-}$ and *ApoE*$^{-/-}$ mice after an intragastric bolus of ^{3}H-cholesterol. In *ApoE*$^{-/-}$*Dgat1*$^{-/-}$ mice, we found a strongly reduced amount of radioactivity in liver and plasma compared with *ApoE*$^{-/-}$ mice (88% and 94%, respectively) with reductions in both non-HDL- (94%) and HDL-cholesterol (91%) concentrations (Fig. 6A, B). The decreased ^{3}H-cholesterol level in the plasma was mainly due to a decreased amount in the VLDL/chylomicron fraction (Fig. 6C). ^{3}H-cholesterol in the small intestine of *ApoE*$^{-/-}$*Dgat1*$^{-/-}$ mice was 82% reduced (Fig. 6D). Together with increased intestinal TC levels these results demonstrate that *ApoE*$^{-/-}$*Dgat1*$^{-/-}$ mice have impaired cholesterol absorption efficiency through the intestine and into plasma and liver. To assess the role of DGAT1 within enterocytes in the uptake of luminal cholesterol, we determined fractional cholesterol absorption using the fecal dual-isotope method. As shown in Fig. 6E, fractional absorption was 32% decreased in *ApoE*$^{-/-}$*Dgat1*$^{-/-}$ mice, indicating that enterocyte DGAT1 affects luminal cholesterol absorption. Intestinal mRNA expression of Abca1, Abcg1, Abcg5, Abcg8, Npc1l1 and Sr-b1 showed no significant differences between both genotypes fed chow diet (supplemental Fig. S6A). In intestines isolated from WTD-fed *ApoE*$^{-/-}$*Dgat1*$^{-/-}$ mice mRNA levels of Abca1 and Npc1l1 were slightly increased, whereas Abcg1 and Sr-b1 were decreased (35% and by 22%, respectively) (supplemental Fig. S6B).

Finally, we examined hepatic and intestinal cholesterol synthesis by measuring the incorporation of ^{14}C-acetate into cholesterol. Hepatic cholesterol synthesis was equivalent in *ApoE*$^{-/-}$*Dgat1*$^{-/-}$ and *ApoE*$^{-/-}$ mice (Fig. 6F), whereas intestinal cholesterol synthesis was 1.5-fold increased in *ApoE*$^{-/-}$*Dgat1*$^{-/-}$ compared with *ApoE*$^{-/-}$ mice (Fig. 6G).

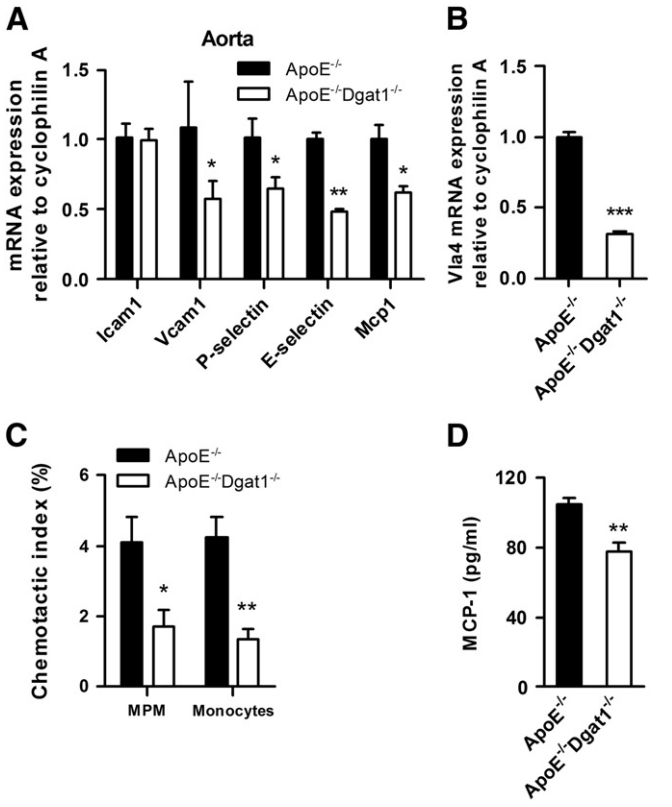

Fig. 2. Reduced monocyte recruitment in *ApoE*$^{-/-}$*Dgat1*$^{-/-}$ mice. Total RNA was isolated from (A) aortas and (B) peritoneal macrophages of chow diet-fed animals. mRNA levels of target genes were determined by real time PCR including normalization to cyclophilin A. Expression of target genes in *ApoE*$^{-/-}$ aorta and macrophages was arbitrarily set to 1. Data represent mean values ($n=6$) ± SEM. (C) Peritoneal macrophages (MPM) and bone marrow-derived monocytes were added to the upper chamber of transwell plates and allowed to migrate through the membrane into the lower chamber containing DMEM and monocyte chemotactic protein-1 (MCP-1; 50 ng/ml). Cells were incubated for 4 h at 37 °C. Migrated cells were counted by flow cytometry. The chemotactic index was calculated from the ratio of the cells that had moved in the presence and absence of MCP-1. Data show the mean values ($n=5$) of two independent experiments ± SEM. (D) MCP-1 concentrations in the serum were determined by ELISA. Data represent mean values ($n=6$–9) ± SEM. $^{*}p<0.05$; $^{**}p\leq0.01$; $^{***}p\leq0.001$.

5. Discussion

Atherosclerotic arteries exhibit cellular and biochemical features of inflammation [19] implying that atherosclerosis is a chronic inflammatory disease [20]. *Dgat1*$^{-/-}$ mice exhibit reduced inflammatory markers in adipose tissue [7]. It has been speculated that whole-body DGAT1 deficiency is associated with reduced inflammation due to the absence of DGAT1 in white adipose tissue, whereas DGAT1 deficiency in macrophages increases the disposition to FA-induced inflammation [7]. We therefore assessed the atherosclerosis susceptibility of an atherosclerotic mouse model lacking DGAT1 in the whole body. For our studies we used female *ApoE*$^{-/-}$ and *ApoE*$^{-/-}$*Dgat1*$^{-/-}$ mice. It is well established that there is a sex-specific difference in atherosclerotic plaque formation between male and female *ApoE*$^{-/-}$ mice with females being more prone to lesion formation [21]. The plasma lipid profile was markedly attenuated in *ApoE*$^{-/-}$*Dgat1*$^{-/-}$ compared with *ApoE*$^{-/-}$ mice with highly reduced TG and substantially reduced TC and FC concentrations, highlighting the importance of DGAT1 in the metabolic context of atherosclerosis.

ApoE$^{-/-}$*Dgat1*$^{-/-}$ mice had reduced plaque development in the aorta and in aortic valve sections after WTD feeding. The number of macrophages within *ApoE*$^{-/-}$*Dgat1*$^{-/-}$ lesions was reduced, indicating a decreased infiltration of monocytes. Infiltrating macrophages take up excessive lipids, become foam cells and are mainly responsible for the necrotic core formations resulting in plaque destabilization. The macrophage represents the link between intracellular cholesterol accumulation and activation of the inflammatory pathway as these cells have both scavenging and immunologic functions [19]. Cell leukocyte and endothelial adhesion molecules (along with chemoattractant and activator molecules) mediate the migration of leukocytes during an inflammatory response, thereby determining the susceptibility to atherosclerotic fatty streak formations [22–24]. The reduced expression of adhesion molecules in the aorta and decreased plasma MCP-1 concentration in *ApoE*$^{-/-}$*Dgat1*$^{-/-}$ mice correlates with the observed reduced atherosclerosis susceptibility. The Vcam-1/Vla-4 pathway, which mediates rolling and firm adhesion in leukocyte transendothelial migration [25,26], was decreased in *ApoE*$^{-/-}$*Dgat1*$^{-/-}$ mice. In accordance, migration efficiencies of *ApoE*$^{-/-}$*Dgat1*$^{-/-}$ monocytes to MCP-1 were reduced.

To investigate the role of macrophages with regard to reduced atherosclerosis susceptibility of *ApoE*$^{-/-}$*Dgat1*$^{-/-}$ mice in more detail, we determined macrophage cholesterol efflux as the initial step in the reverse cholesterol transport. Increased expression of ABCA1, ABCG1 and SR-B1 as well as increased cholesterol efflux from *ApoE*$^{-/-}$*Dgat1*$^{-/-}$ compared with *ApoE*$^{-/-}$ and *Dgat1*$^{-/-}$ compared with Wt macrophages indicated that (independent of the background) DGAT1 deficiency positively influences cholesterol efflux, which is generally associated with an anti-atherosclerotic phenotype. Both increased cholesterol efflux and decreased lipoprotein uptake are important features in reducing macrophage lipid accumulation. In accordance, macrophages from *ApoE*$^{-/-}$*Dgat1*$^{-/-}$ mice were resistant to lipid droplet accumulation by acLDL and VLDL loading, which was consistent with reduced lipoprotein lipase (data not shown) and DGAT activities. Sr-a mRNA expression was downregulated in acLDL-loaded macrophages and might be the cause for the reduced uptake of modified LDL in the absence of DGAT1 and a decreased foamy phenotype of macrophages isolated from WTD-fed *ApoE*$^{-/-}$*Dgat1*$^{-/-}$ mice.

ApoE$^{-/-}$*Dgat1*$^{-/-}$ mice showed reduced lipid accumulation in the liver but markedly increased TG and cholesterol content in the small intestine. These findings indicate that DGAT1 deficiency in enterocytes has an impact on intestinal cholesterol absorption and therefore might lead to lower plasma cholesterol levels. A complex interplay between the liver and the intestine determines plasma cholesterol concentrations. The liver regulates synthesis, secretion and clearance of cholesterol-rich lipoproteins and determines the amount of cholesterol eliminated into the bile, either as cholesterol or after conversion to bile acids. The intestine plays a key role in regulating the net balance of cholesterol by serving as the site of both absorption of dietary cholesterol and reabsorption of biliary cholesterol. Thus, cholesterol is either absorbed by the intestine or excreted into the feces. DGAT1 deficiency affected intestinal TG metabolism in *ApoE*$^{-/-}$ mice when the dietary load of fat was high, comparable with *Dgat1*$^{-/-}$ mice [6]. *Dgat1*$^{-/-}$ mice have reduced postprandial triglyceridemic response with less chylomicron release from the intestine compared with Wt mice. In accordance, *ApoE*$^{-/-}$*Dgat1*$^{-/-}$ mice accumulated lipid droplets in the jejunum when fed a WTD rich in saturated FAs, suggesting that DGAT2 and diacylglycerol transacylase contribute to intestinal TG synthesis in the absence of DGAT1 [6]. DGAT1 deficiency, however, reduced WTD-induced hepatic steatosis in *ApoE*$^{-/-}$ mice. A similar reduction in liver steatosis, which involves the uptake of dietary FAs and the activation of FA synthesis, was observed in *Dgat1*$^{-/-}$ mice after a 3-week challenge with high fat diet [27]. The authors reported a decrease of hepatic TG concentrations by 80% compared with Wt mice. In the same publication hepatic deletion of DGAT1 was shown to reduce TG concentrations in the liver by 50% [27], whereas intestine-specific expression of DGAT1 reversed resistance to diet-induced hepatic steatosis in *Dgat1*$^{-/-}$ mice [8]. Thus, increased TG and TC concentrations and lipid droplet accumulation in the intestines of *ApoE*$^{-/-}$*Dgat1*$^{-/-}$ mice indicate that intestinal DGAT1

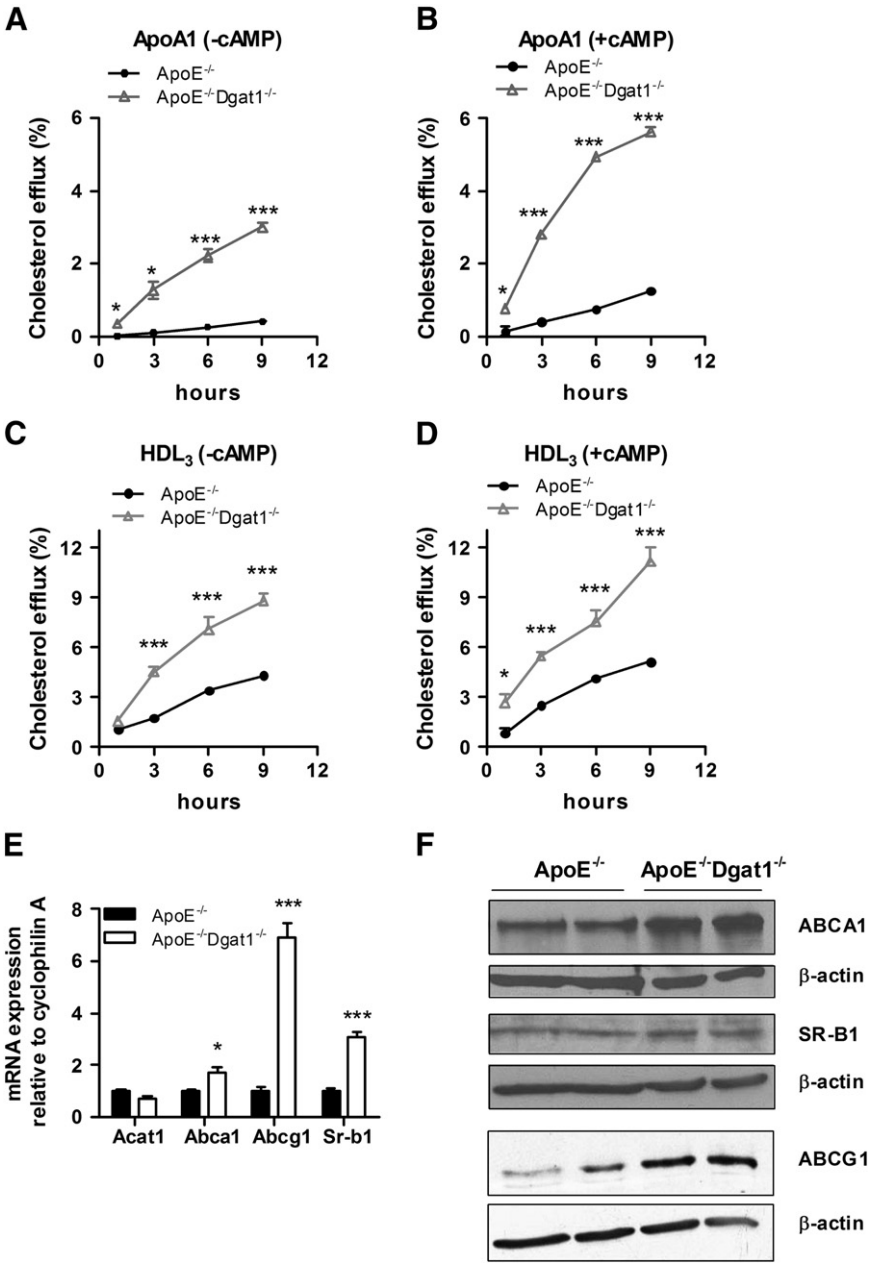

Fig. 3. Increased cholesterol efflux from *ApoE*$^{-/-}$*Dgat1*$^{-/-}$ macrophages. Macrophages from chow diet-fed *ApoE*$^{-/-}$ and *ApoE*$^{-/-}$*Dgat1*$^{-/-}$ mice were labeled with ^{3}H-cholesterol and cholesterol efflux to (A,B) ApoA1 and (C,D) HDL_3 was assessed in the (A,C) absence and (B,D) presence of 8-bromo-cAMP. Cholesterol efflux was expressed as the percentage of ^{3}H-cholesterol transferred from cells to the medium. Data show the mean values ($n = 4–6$) ± SEM of triplicate repeats. (E) Total RNA was isolated from acLDL-loaded macrophages. mRNA expression of target genes was determined by real time PCR including normalization to cyclophilin A. Expression of target genes in *ApoE*$^{-/-}$ foam cells was arbitrarily set to 1. Data represent mean values ($n = 6$) ± SEM. (F) Cell extracts of foam cells (40 μg per lane) were separated by SDS-PAGE. Protein expression of ABCA1, SR-B1 and ABCG1 were analyzed by Western blotting relative to the expression of β-actin. $^{*}p<0.05$; $^{***}p\leq0.001$.

stimulates chylomicron secretion out of enterocytes, thereby controlling TG and TC release.

We found markedly decreased acute cholesterol uptake in the small intestine of *ApoE*$^{-/-}$*Dgat1*$^{-/-}$ mice and almost absent radioactivity in plasma and liver 4 h after an intragastric bolus of ^{3}H-cholesterol. Absence of DGAT1 also resulted in reduced fractional cholesterol absorption as determined by the fecal dual-isotope method. These results indicate that intestinal DGAT1 markedly affects dietary cholesterol uptake. In intestines isolated from WTD-fed ApoE$^{-/-}$Dgat1$^{-/-}$ mice mRNA levels of Abca1 and Npc1l1 were slightly increased, whereas Abcg1 and Sr-b1 were slightly decreased. All differences, however, were less than 1.5-fold up- or downregulated, indicating that changes in mRNA levels might not explain the phenotype of ApoE$^{-/-}$Dgat1$^{-/-}$ intestines.

Our findings are in accordance with reduced cholesterol absorption observed in genetically obese high fat diet-fed KKA^{y} mice treated with a DGAT1-specific inhibitor [18]. We suggest that in the absence of DGAT1, less cholesterol accumulates in the plasma. A similar correlation between a reduced ability of mice to absorb intestinal cholesterol and decreased atherosclerotic lesion formation has been demonstrated in *ApoE*$^{-/-}$ mice lacking the cholesterol transporter Niemann–Pick C1 Like 1 [16]. Our data indicate that less cholesterol uptake increases intestinal cholesterol biosynthesis, which was also demonstrated in Niemann–Pick C1 Like 1-deficient mice [16]. We hypothesize that due to reduced secretion of chylomicrons from *ApoE*$^{-/-}$*Dgat1*$^{-/-}$ enterocytes, cholesterol resides within the small intestine, resulting in decreased plasma TG and cholesterol concentrations, which contributes to the attenuation of plaque formation in these mice.

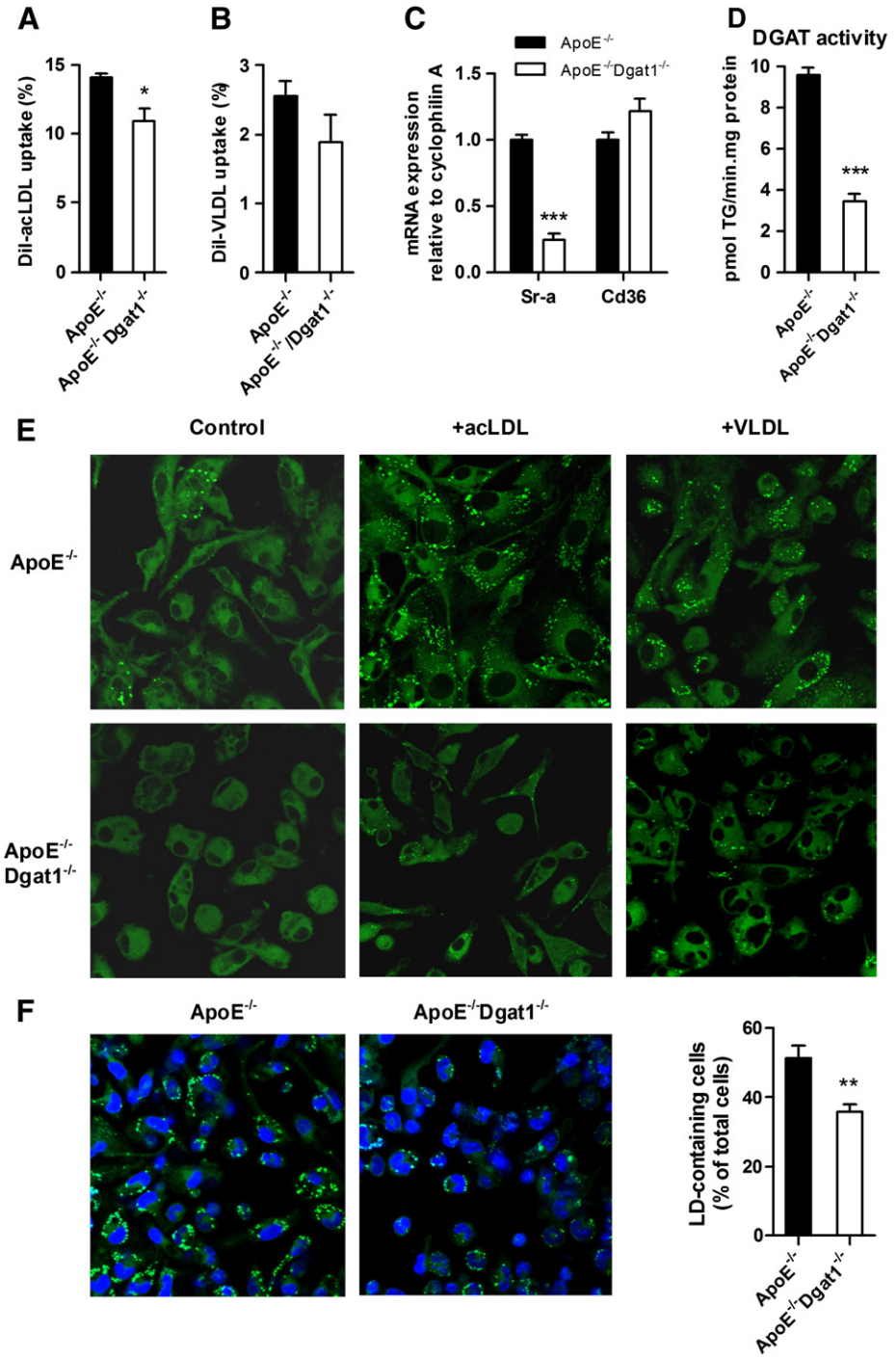

Fig. 4. Reduced foam cell formation of *ApoE*$^{-/-}$*Dgat1*$^{-/-}$ macrophages. (A,B) Macrophages from chow diet-fed *ApoE*$^{-/-}$ and *ApoE*$^{-/-}$*Dgat1*$^{-/-}$ mice were cultured for 24 h in DMEM/10% LPDS. Cells were then incubated for 4 h in serum-free DMEM with (A) 10 μg/ml 1,1′-dioctadecyl-3,3,3′,3′-tetramethylindocarbocyanine perchlorate (DiI)-acLDL or (B) 50 μg/ml DiI-VLDL. Cells were washed, detached, stained with F4/80 antibody and analyzed by fluorescence activated cell sorting. Data show the mean values ($n=3$) ± SEM. (C) Total RNA was isolated from acLDL-loaded macrophages. mRNA levels of Sr-a and Cd36 were determined by real time PCR including normalization to cyclophilin A. Expression of target genes in *ApoE*$^{-/-}$ foam cells was arbitrarily set to 1. Data represent mean values ($n=6$) ± SEM. (D) DGAT activity was determined in 50 μg macrophage lysates using 200 μM sn-1,2-dioleoylglycerol and 25 μM ^{14}C-oleoyl-CoA (ARC Inc., St. Louis, MO) as substrates and 10 mM $MgCl_2$. Data show the mean values ($n=4$) ± SEM. (E) Representative images of Nile red-stained control, acLDL-and VLDL-loaded macrophages. Lipid droplets were visualized by confocal laser scanning microscopy. Original magnification, ×63. (F) *ApoE*$^{-/-}$ and *ApoE*$^{-/-}$*Dgat1*$^{-/-}$ mice were fed a WTD for 9 weeks. Macrophages were isolated, cultured for 2 h in serum-free DMEM and stained with Nile Red. Data represent the percent ± SEM of lipid droplet-containing cells from at least 500 cells per genotype. $^{*}p<0.05$; $^{**}p\leq0.01$; $^{***}p\leq0.001$.

6. Conclusions

DGAT1 inhibitors were shown to induce weight loss and improve insulin sensitivity, glucose tolerance and lipid levels in obese animals [28,29], suggesting that DGAT1 inhibitors may be beneficial drugs to treat obesity, diabetes and dyslipidemia. Here we demonstrate that the lack of DGAT1 decreases atherosclerotic plaque formation. Contributing factors include reduced macrophage migration and aortic inflammation, increased cholesterol efflux from macrophages, and decreased cholesterol uptake and absorption. We conclude that different mechanisms are operative in macrophages and intestine. In macrophages lacking DGAT1, the

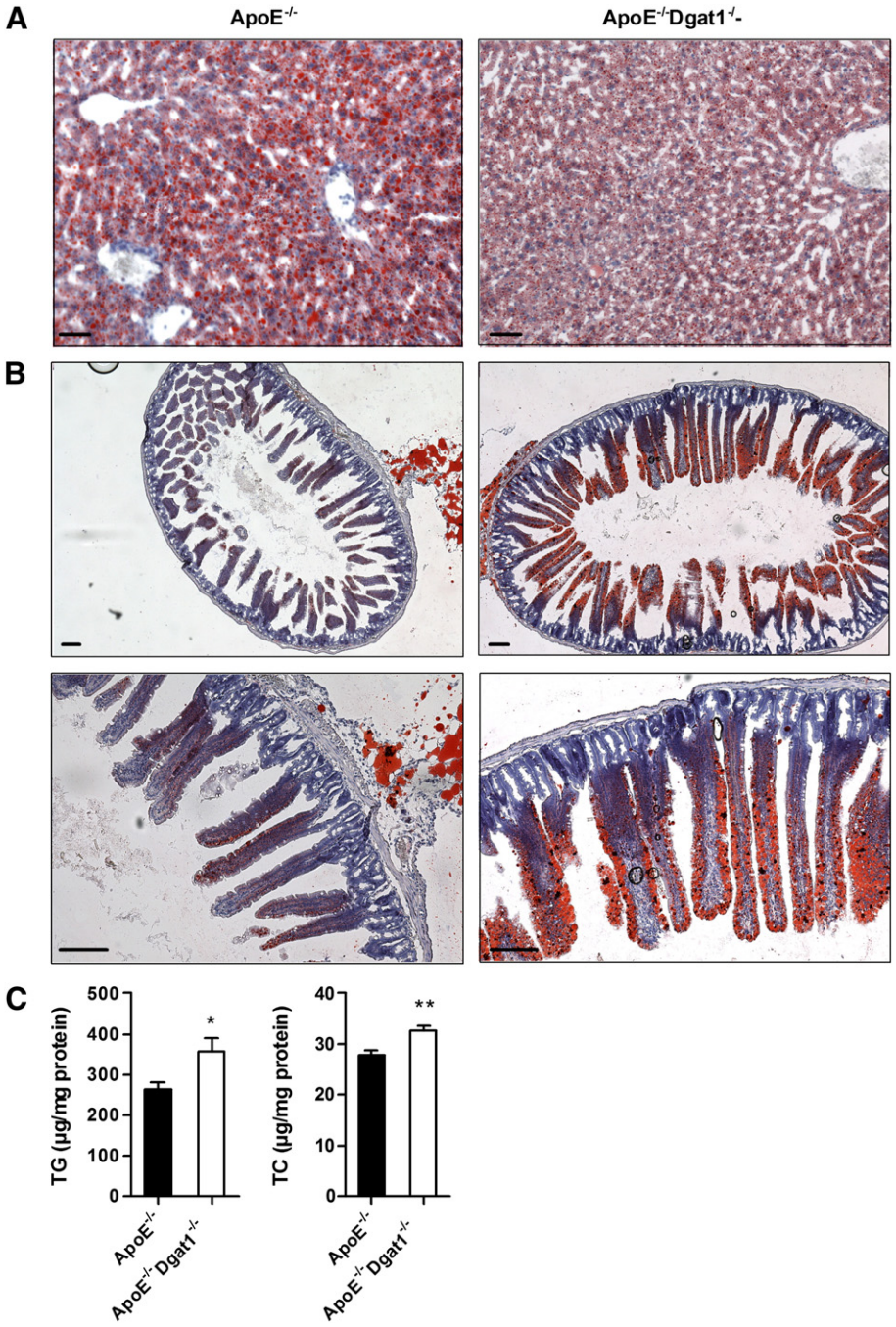

Fig. 5. Number of lipid droplets are reduced in liver but increased in intestine of *ApoE*$^{-/-}$*Dgat1*$^{-/-}$ mice. *ApoE*$^{-/-}$ and *ApoE*$^{-/-}$*Dgat1*$^{-/-}$ mice were fed a WTD for 9 weeks. Representative images of oil red O-stained sections of (A) liver and (B) intestine. Lipid droplets were visualized using a Nikon Eclipse 80i microscope. A,B, upper lane: original magnification, ×4; B, lower lane: original magnification, ×10. Scale bars: 500 µm. (C) Intestinal TG ($n=3$) and TC ($n=4$) concentrations were determined enzymatically. Values are means ± SEM. $^{**}p<0.01$.

reduced uptake of modified lipoproteins and the increased efflux of cholesterol result in markedly reduced foam cell formation. In addition to the reduced mobility of these macrophages this leads to less inflammation in the aorta and reduced atherosclerotic plaque formation. The uptake and absorption of cholesterol are markedly reduced in *ApoE*$^{-/-}$*Dgat1*$^{-/-}$ mice, leading to increased cholesterol biosynthesis. The decrease in plasma lipid parameters (including cholesterol) and elevated intestinal cholesterol concentrations are likely a result of less secretion of chylomicrons from *ApoE*−/− *Dgat1*−/− intestines. Although the respective roles of DGAT1 in macrophage function versus intestinal lipid absorption with respect to atherosclerotic plaque formation are still unknown, our study provides strong evidence that whole-body DGAT1 deficiency is atheroprotective, implicating an additional application of DGAT1 inhibitors.

Acknowledgments

This work was supported by the Austrian Science Fund (SFB-LIPOTOX F30, DK-MCD W1226, P19186 and P22832) and the Austrian Federal Ministry of Science and Research (GEN-AU project Genomics of Lipid-associated Disorders III—GOLDIII). P.G.C., S.O. and E.A. are fellows of the PhD Program Molecular Medicine of the Medical University of Graz. The authors thank R.V. Farese Jr. for providing the *Dgat1*$^{-/-}$ mice, S. Schauer and A. Ibovnik for excellent technical assistance and I. Hindler for mice care.

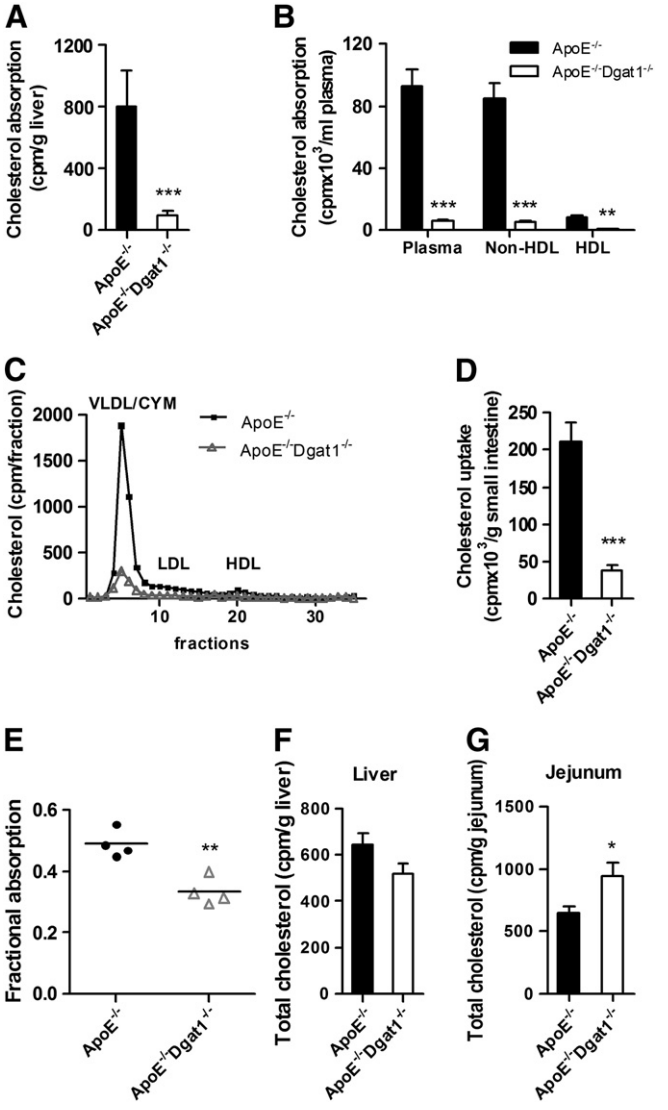

Fig. 6. Decreased cholesterol absorption in *ApoE*$^{-/-}$*Dgat1*$^{-/-}$ mice. Mice were gavaged with 200 μl corn oil containing 2 μCi ^{3}H-cholesterol and 0.2 mg cholesterol. 4 h later, absorption in (A) liver and (B) plasma and (D) intestinal uptake of ^{3}H-cholesterol was determined by liquid scintillation counting. ^{3}H-Cholesterol in HDL was assayed after precipitation of ApoB-containing lipoproteins using Quantolip HDL (Technoclone GmbH). (C) Plasma samples from each genotype ($n=6$) were pooled and 200 μl were subjected to fast protein liquid chromatography using a Superose 6 column. ^{3}H-Cholesterol in each fraction was determined by liquid scintillation counting. (E) Fractional cholesterol absorption was determined using the fecal dual-isotope method. Cholesterol biosynthesis in (F) liver and (G) jejunum was determined 1 h after ^{14}C-acetate administration. Data represent mean values ($n=4$–5) ± SEM. $^{*}p<0.05$; $^{**}p\leq0.01$; $^{***}p\leq0.001$.

Appendix A. Supplementary data

Supplementary data to this article can be found online at doi:10.1016/j.bbalip.2011.08.010.

References

[1] S. Cases, S.J. Smith, Y.W. Zheng, H.M. Myers, S.R. Lear, E. Sande, S. Novak, C. Collins, C.B. Welch, A.J. Lusis, S.K. Erickson, R.V. Farese Jr., Identification of a gene encoding an acyl CoA:diacylglycerol acyltransferase, a key enzyme in triacylglycerol synthesis, Proc Natl Acad Sci USA 95 (1998) 13018–13023.
[2] S. Cases, S.J. Stone, P. Zhou, E. Yen, B. Tow, K.D. Lardizabal, T. Voelker, R.V. Farese Jr., Cloning of DGAT2, a second mammalian diacylglycerol acyltransferase, and related family members, J Biol Chem 276 (2001) 38870–38876.
[3] C.L. Yen, M. Monetti, B.J. Burri, R.V. Farese Jr., The triacylglycerol synthesis enzyme DGAT1 also catalyzes the synthesis of diacylglycerols, waxes, and retinyl esters, J Lipid Res 46 (2005) 1502–1511.
[4] S.J. Stone, H.M. Myers, S.M. Watkins, B.E. Brown, K.R. Feingold, P.M. Elias, R.V. Farese Jr., Lipopenia and skin barrier abnormalities in DGAT2-deficient mice, J Biol Chem 279 (2004) 11767–11776.
[5] S.J. Smith, S. Cases, D.R. Jensen, H.C. Chen, E. Sande, B. Tow, D.A. Sanan, J. Raber, R.H. Eckel, R.V. Farese Jr., Obesity resistance and multiple mechanisms of triglyceride synthesis in mice lacking Dgat, Nat Genet 25 (2000) 87–90.
[6] K.K. Buhman, S.J. Smith, S.J. Stone, J.J. Repa, J.S. Wong, F.F. Knapp Jr., B.J. Burri, R.L. Hamilton, N.A. Abumrad, R.V. Farese Jr., DGAT1 is not essential for intestinal triacylglycerol absorption or chylomicron synthesis, J Biol Chem 277 (2002) 25474–25479.
[7] S.K. Koliwad, R.S. Streeper, M. Monetti, I. Cornelissen, L. Chan, K. Terayama, S. Naylor, M. Rao, B. Hubbard, R.V. Farese Jr., DGAT1-dependent triacylglycerol storage by macrophages protects mice from diet-induced insulin resistance and inflammation, J Clin Invest 120 (2010) 756–767.
[8] B. Lee, A.M. Fast, J. Zhu, J.X. Cheng, K.K. Buhman, Intestine-specific expression of acyl CoA:diacylglycerol acyltransferase 1 reverses resistance to diet-induced hepatic steatosis and obesity in Dgat1−/− mice, J Lipid Res 51 (2010) 1770–1780.
[9] P. Libby, Inflammation in atherosclerosis, Nature 420 (2002) 868–874.
[10] E.A. Kaperonis, C.D. Liapis, J.D. Kakisis, D. Dimitroulis, V.G. Papavassiliou, Inflammation and atherosclerosis, Eur J Vasc Endovasc Surg 31 (2006) 386–393.
[11] S.H. Zhang, R.L. Reddick, J.A. Piedrahita, N. Maeda, Spontaneous hypercholesterolemia and arterial lesions in mice lacking apolipoprotein E, Science 258 (1992) 468–471.
[12] A.S. Plump, J.D. Smith, T. Hayek, K. Aalto-Setala, A. Walsh, J.G. Verstuyft, E.M. Rubin, J.L. Breslow, Severe hypercholesterolemia and atherosclerosis in apolipoprotein E-deficient mice created by homologous recombination in ES cells, Cell 71 (1992) 343–353.
[13] A. Kratzer, M. Buchebner, T. Pfeifer, T.M. Becker, G. Uray, M. Miyazaki, S. Miyazaki-Anzai, B. Ebner, P.G. Chandak, R.S. Kadam, E. Calayir, N. Rathke, H. Ahammer, B. Radovic, M. Trauner, G. Hoefler, U.B. Kompella, G. Fauler, M. Levi, S. Levak-Frank, G.M. Kostner, D. Kratky, Synthetic LXR agonist attenuates plaque formation in apoE−/− mice without inducing liver steatosis and hypertriglyceridemia, J Lipid Res 50 (2009) 312–326.
[14] S.K. Basu, J.L. Goldstein, G.W. Anderson, M.S. Brown, Degradation of cationized low density lipoprotein and regulation of cholesterol metabolism in homozygous familial hypercholesterolemia fibroblasts, Proc Natl Acad Sci USA 73 (1976) 3178–3182.
[15] P.G. Chandak, B. Radovic, E. Aflaki, D. Kolb, M. Buchebner, E. Frohlich, C. Magnes, F. Sinner, G. Haemmerle, R. Zechner, I. Tabas, S. Levak-Frank, D. Kratky, Efficient phagocytosis requires triacylglycerol hydrolysis by adipose triglyceride lipase, J Biol Chem 285 (2010) 20192–20201.
[16] H.R. Davis Jr., L.M. Hoos, G. Tetzloff, M. Maguire, L.J. Zhu, M.P. Graziano, S.W. Altmann, Deficiency of Niemann–Pick C1 Like 1 prevents atherosclerosis in ApoE−/− mice, Arterioscler Thromb Vasc Biol 27 (2007) 841–849.
[17] L.R. Brunham, J.K. Kruit, J. Iqbal, C. Fievet, J.M. Timmins, T.D. Pape, B.A. Coburn, N. Bissada, B. Staels, A.K. Groen, M.M. Hussain, J.S. Parks, F. Kuipers, M.R. Hayden, Intestinal ABCA1 directly contributes to HDL biogenesis in vivo, J Clin Invest 116 (2006) 1052–1062.
[18] T. Yamamoto, H. Yamaguchi, H. Miki, M. Shimada, Y. Nakada, M. Ogino, K. Asano, K. Aoki, N. Tamura, M. Masago, K. Kato, Coenzyme A: diacylglycerol acyltransferase 1 inhibitor ameliorates obesity, liver steatosis, and lipid metabolism abnormality in KKAy mice fed high-fat or high-carbohydrate diets, Eur J Pharmacol 640 (2010) 243–249.
[19] M.F. Linton, S. Fazio, Macrophages, inflammation, and atherosclerosis, Int J Obes Relat Metab Disord 27 (Suppl 3) (2003) S35–S40.
[20] R. Ross, Atherosclerosis—an inflammatory disease, N Engl J Med 340 (1999) 115–126.
[21] G. Caligiuri, A. Nicoletti, X. Zhou, I. Tornberg, G.K. Hansson, Effects of sex and age on atherosclerosis and autoimmunity in apoE-deficient mice, Atherosclerosis 145 (1999) 301–308.
[22] T.A. Springer, Traffic signals for lymphocyte recirculation and leukocyte emigration: the multistep paradigm, Cell 76 (1994) 301–314.
[23] M.F. Nageh, E.T. Sandberg, K.R. Marotti, A.H. Lin, E.P. Melchior, D.C. Bullard, A.L. Beaudet, Deficiency of inflammatory cell adhesion molecules protects against atherosclerosis in mice, Arterioscler Thromb Vasc Biol 17 (1997) 1517–1520.
[24] Z.M. Dong, S.M. Chapman, A.A. Brown, P.S. Frenette, R.O. Hynes, D.D. Wagner, The combined role of P- and E-selectins in atherosclerosis, J Clin Invest 102 (1998) 145–152.
[25] M.J. Elices, L. Osborn, Y. Takada, C. Crouse, S. Luhowskyj, M.E. Hemler, R.R. Lobb, VCAM-1 on activated endothelium interacts with the leukocyte integrin VLA-4 at a site distinct from the VLA-4/fibronectin binding site, Cell 60 (1990) 577–584.
[26] R. Alon, P.D. Kassner, M.W. Carr, E.B. Finger, M.E. Hemler, T.A. Springer, The integrin VLA-4 supports tethering and rolling in flow on VCAM-1, J Cell Biol 128 (1995) 1243–1253.
[27] C.J. Villanueva, M. Monetti, M. Shih, P. Zhou, S.M. Watkins, S. Bhanot, R.V. Farese Jr., Specific role for acyl CoA:Diacylglycerol acyltransferase 1 (Dgat1) in hepatic steatosis due to exogenous fatty acids, Hepatology 50 (2009) 434–442.
[28] A.M. Birch, S. Birtles, L.K. Buckett, P.D. Kemmitt, G.J. Smith, T.J. Smith, A.V. Turnbull, S.J. Wang, Discovery of a potent, selective, and orally efficacious pyrimidinooxazinyl bicyclooctaneacetic acid diacylglycerol acyltransferase-1 inhibitor, J Med Chem 52 (2009) 1558–1568.
[29] G. Zhao, A.J. Souers, M. Voorbach, H.D. Falls, B. Droz, S. Brodjian, Y.Y. Lau, R.R. Iyengar, J. Gao, A.S. Judd, S.H. Wagaw, M.M. Ravn, K.M. Engstrom, J.K. Lynch, M.M. Mulhern, J. Freeman, B.D. Dayton, X. Wang, N. Grihalde, D. Fry, D.W. Beno, K.C. Marsh, Z. Su, G.J. Diaz, C.A. Collins, H. Sham, R.M. Reilly, M.E. Brune, P.R. Kym, Validation of diacyl glycerolacyltransferase I as a novel target for the treatment of obesity and dyslipidemia using a potent and selective small molecule inhibitor, J Med Chem 51 (2008) 380–383.